RSC Advances

RSC Publishing

COMMUNICATION

View Article Online
View Journal | View Issue

An *ab initio* explanation of the activation and antagonism strength of an AMPA-sensitive glutamate receptor

Cite this: *RSC Advances*, 2013, **3**, 14988

Received 1st May 2013,
Accepted 20th July 2013

DOI: 10.1039/c3ra42149j

www.rsc.org/advances

Ana Caroline V. Martins,*[a] Pedro de Lima-Neto,[a] Ito L. Barroso-Neto,[b] Benildo S. Cavada,[b] Valder N. Freire[c] and Ewerton W. S. Caetano[d]

We report quantum biochemistry calculations focusing on the binding pocket of the glutamate receptor co-crystallized with agonists (full and partial) and a antagonist. The calculated electronic binding energy follows the order AMPA > glutamate > kainate > DNQX, which explains published experimental data on GluR2 activation and antagonism strength.

Glutamatergic receptors (GluRs) are an important group of ion channels in the central nervous system (CNS). They are found in fast excitatory synapses and are related to important functions like learning and memory.[1] GluRs are classified according to their responses to three amino acids: N-methyl-D-aspartic acid (NMDA), α-amino-3-hydroxy-5-methyl-4-isoxazole propionic acid (AMPA) and kainic acid (Kainate). Each receptor is formed by four subunits which are not necessarily equal.[2,3] Activation, or agonism, and antagonism of these receptors are associated with the opening, or not, of the ion channel.[4] In crystallographic data of a specific AMPA receptor subunit, GluR2, it is observed that, in comparison with the apo state, there is a high degree of closure of the ligand binding domain (LBD) when an agonist is present. In contrast, a very self-effacing closure is observed if the agonist is replaced by an antagonist. The first result to suggest this relation was obtained in the comparison of the closure of GluR2 caused by the four ligands: glutamate = AMPA (full agonists) > kainate (partial agonist) > DNQX (the antagonist 6,7-dinitroquinoxaline-2,3-dione).[5] Since then, it has been confirmed that the degree of LBD closure caused by a ligand is directly related to the agonism/antagonism of the latter.[6] Starting from the analysis of crystallographic data it was also possible to infer the importance of the residues for interaction with protein ligands, with the residue Arg485 being the most important in the ligand–GluR2 interaction. Other residues have been shown to be important for the GluR2 interaction with its total and partial agonists: Tyr450, Thr480, Ser652, Ser654, Thr655, Pro478 and Glu705. On the other hand, for the antagonist DNQX, other residues are considered important: Tyr450, Pro478, Thr480, Thr686 and Tyr732.[5]

After the achievement of the co-crystallization of GluR2 with its ligands,[5,7] several computational studies were carried out. For example, molecular dynamics simulations of the GluR2 LBD were performed to investigate the gating mechanism of the ion channels by the structural changes of the receptors, the ligand-binding processes and the role of water molecules at the binding pocket.[8–16] Some of these studies have reinforced the importance of the residues Thr480, Ser654, Thr655, Pro478, Glu705 and Arg485, with the importance of Arg485 also being shown in studies at the quantum level.[8,10,12,17–19] Studies that adopt a quantum mechanical level are mostly limited, however, to evaluating the properties of the ligands and the importance of water in the binding pocket.[17–20] Nevertheless, with the increase of computational power, it has become feasible to calculate the electronic interaction energies with components of the binding site using density functional theory (DFT).[21]

In this work, we perform DFT quantum calculations to obtain the interaction energy profile for a set of ligands interacting with GluR2 amino acid residues within an enlarged binding pocket. To this end, four ligands were selected: glutamate, AMPA, kainate and DNQX (PDB codes 1FTJ, 1FTM, 1FW0 and 1FTL, respectively). From simulation results, we demonstrate that charged residues far away from the ligand do contribute significantly to the electronic binding interaction. We also show that the electronic binding energies of glutamate, AMPA, kainate and DNQX follow the order of protein activation caused by the ligand (full agonists > partial agonist > antagonist) only when considering all the residues within the enlarged binding pocket. We consider the amino acid residues found inside a sphere with a radius of 10 Å from each ligand. Some amino acid residues are shown for each GluR2–ligand system in Fig. 1. Among them are the most relevant interacting residues.

[a]*Departamento de Química Analítica e Físico-Química, Universidade Federal do Ceará, Campus do Pici, 60455-760 Fortaleza, Ceará, Brazil. E-mail: carolinevmartins@gmail.com; plimaneto@gmail.com*
[b]*Departamento de Bioquímica e Biologia Molecular, Universidade Federal do Ceará, Campus do Pici, 60410-970 Fortaleza, Ceará, Brazil. E-mail: itoliberato@gmail.com; bscavada@gmail.com*
[c]*Departamento de Física, Universidade Federal do Ceará, Centro de Ciências, CP 6030, Campus do Pici, 60455-760 Fortaleza, Ceará, Brazil. E-mail: vnffreire@gmail.com*
[d]*Instituto de Educação, Ciência e Tecnologia do Ceará, 60040-531 Fortaleza, Ceará, Brazil. E-mail: ewcaetano@gmail.com*

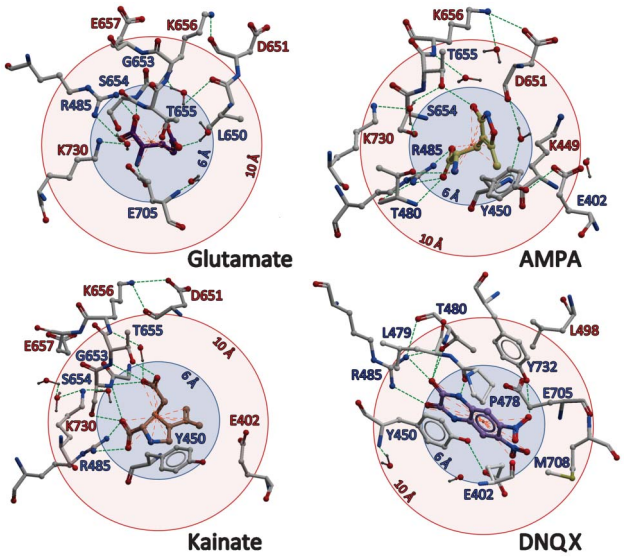

Fig. 1 Amino acid residues inside two interaction regions: a close-neighborhood sphere with a radius of 6 Å (blue) and an interaction shell with radius between 6 and 10 Å (red).

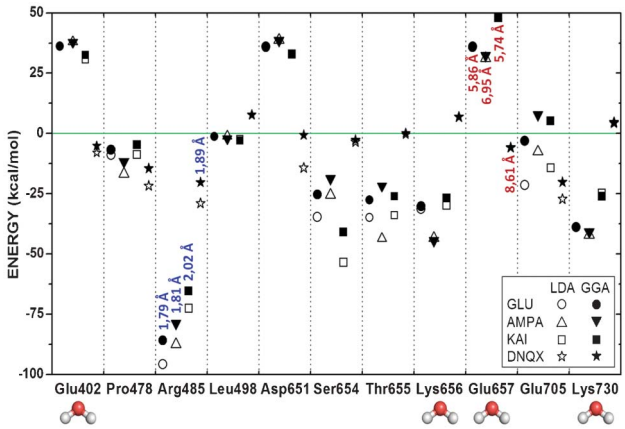

Fig. 2 The interaction energies between the amino acid residues and each ligand. Residues with appended water molecules are also indicated. The distance between the most attractive and the most repulsive residues and the ligands are pointed out in blue and red, respectively.

To achieve a description of the GluR2–ligand system at the quantum level, the molecular fractionation with conjugate caps scheme (MFCC) was adopted. As a matter of fact, the MFCC method has been previously employed for other biological systems successfully,[22–24] allowing one to perform estimates of the interaction energy between the ligand L with GluR2 neighbor residues Ri, E(L–Ri). Before the interaction energy calculations, the system geometry was set up as follows: hydrogen atoms were added and their positions were optimized classically using the Forcite code and the consistent valence force field (CVFF), which is parameterized for amino acids.[25–27] Non-hydrogen atomic positions were kept fixed, and the protonation states of the amino acid residues were set to physiological pH (7.4). Afterwards, the computations were accomplished using the DMOL3 code within both the local density approximation (LDA, with Perdew–Wang parameterization) and the dispersion corrected generalized gradient approximation (GGA + D, with Perdew–Burke–Ernzerhof parameterization and the semi-empirical correction of dispersion forces of Tkatchenko and Scheffler[28–32]). In order to expand the Kohn–Sham orbitals for all the electrons, a double numerical plus polarization (DNP 4.4) basis set was adopted. The orbital cutoff was set to 3.7 Å and the total energy variation set to achieve convergence was 10^{-6} Ha. All calculations were performed in a vacuum environment.

The interaction energies for a set of residue–ligand pairs are presented in Fig. 2, with the distance between them being indicated. One can see that the LDA electronic binding energies (taken as the negative of the corresponding interaction energies) are always larger than the GGA + D results, as a consequence of the well known trend exhibited by the LDA functional to overestimate interatomic binding forces. Residues with at least one atom inside a 6 Å sphere (close neighbors) centered at the ligand have their centroid–centroid distances indicated in blue. Residues with atoms belonging to the spherical shell with internal radius 6 Å and external radius 10 Å are indicated in red. It is clear that the residues most important for the agonists interact differently in comparison with the antagonist DNQX, for which the largest contribution to the stability of the interaction is due to close neighbor residues, most of them without net charge. In contrast, for the system with the agonists, uncharged residues are important only if they are very close to the ligand, with the charged residues Asp651, Glu657 and Lys730 in the same neighborhood exhibiting strong interaction energies.

Table 1 depicts the interaction regions to which each residue belongs and the distance (in brackets) between the centroids of each residue and corresponding ligands. We see that the most important residue for the interaction of all four ligands with GluR2 is Arg485, in agreement with the literature. In the particular case of the GluR2–glutamate pair, in addition to Arg485 (LDA electronic binding energy of approximately 95 kcal mol^{-1}), the other relevant residues (and also in agreement with previous data) are Ser654 (LDA electronic binding energy 35 kcal mol^{-1}) and Thr655 (LDA electronic binding energy 35 kcal mol^{-1}). Besides these, we also see that the amino acid residues Leu650, Lys730,

Table 1 Amino acid residues and their respective interaction layers [distance between the closest atoms of the ligand and the residue]

Residue	$d[r]_{GLU}$ (Å)	$d[r]_{AMPA}$ (Å)	$d[r]_{KAI}$ (Å)	$d[r]_{DNQX}$ (Å)
Glu705	3.5 [1.70]	3.0 [3.04]	4.5 [2.26]	3.5 [2.74]
Ser654	3.0 [1.86]	4.5 [1.93]	4.5 [1.64]	7.5 [4,71]
Thr655	4.5 [1.75]	5.0 [1.53]	5.5 [1.66]	8.5 [3.00]
Pro478	4.5 [1.91]	4.5 [1.90]	5.0 [2.13]	4.5 [1.74]
Arg485	5.0 [1.79]	6.0 [1.81]	5.5 [2.02]	6.0 [1.98]
Lys656	6.5 [3.89]	7.5 [4.98]	7.5 [3.88]	11.0 [8.21]
Glu402	6.5 [4.48]	6.0 [3.04]	6.5 [2.87]	5.0 [2.40]
Leu498	6.5 [4.76]	6.5 [4.57]	8.0 [5.05]	6.5 [4.93]
Lys730	6.5 [5.24]	7.0 [5.29]	8.0 [5.31]	7.0 [6.42]
Glu657	8.0 [5.86]	9.5 [6.95]	9.0 [5.74]	12.5 [8.61]
Asp651	9.0 [6.87]	8.0 [5.58]	9.5 [7.00]	12.5 [9.54]

Lys656, Glu657 and Asp651 cannot be neglected. Indeed, not all residues usually deemed as relevant are worth mentioning. For GluR2–AMPA the interaction energy results are similar to those obtained for GluR2–glutamate. We note the relative importance of Ser654 (electronic binding energy 27 kcal mol^{-1}) and Thr655, as well as the residues Lys730, Lys656, Lys449, Arg684, Glu402 and Asp651. For the interaction between GluR2 and kainate, in addition to Arg485 (electronic binding energy 70 kcal mol^{-1}), the only residue mentioned in the literature that we have found to be relevant is Ser656. But we have observed that residues Glu402, Glu657 and Asp651 also deserve to be taken into account. Finally, for the GluR2–DNQX interaction, we have a relevant role assigned to Pro478 (also in agreement with the literature, electronic binding energy 21 kcal mol^{-1}) and, as this was not suggested previously, we also have significant contributions from Glu705 (LDA electronic binding energy 28 kcal mol^{-1}).[5]

Once the MFCC was applied to each residue within a given interaction region, it was possible to evaluate the total interaction energy for the GluR2–ligand system considering the close neighbor sphere only (radius smaller than 6 Å) and the enlarged sphere obtained by including the interaction shell between 6 and 10 Å. It is expected that close neighbor residues have a dominant contribution. According to our calculations, however, to consider only close neighbor residues is not enough to provide a good description of the system, because it does not agree with the experimentally observed agonism or antagonism of the ligands, especially in relation to total and partial agonism. For residues inside a spherical binding pocket with a radius of 6 Å, the total interaction energy follows the order glutamate > kainate > AMPA > DNQX. The partial agonist kainate binds to GluR2 (electronic binding energy −310 kcal mol^{-1}, LDA, and −217 kcal mol^{-1}, GGA + D) more strongly than AMPA (electronic binding energy −280 kcal mol^{-1}, LDA, −185 kcal mol^{-1}, GGA + D), which is a full agonist, as shown in Fig. 3. However, when residues inside an expanded binding pocket sphere with radius 10 Å are fully taken into account, the sequence becomes AMPA > glutamate > kainate > DNQX. Therefore, the role of the residues more distant from the ligand in the binding pocket is essential to achieve an adequate characterization of the receptor function. Such a result does not depend on the employed functional (LDA or GGA + D).

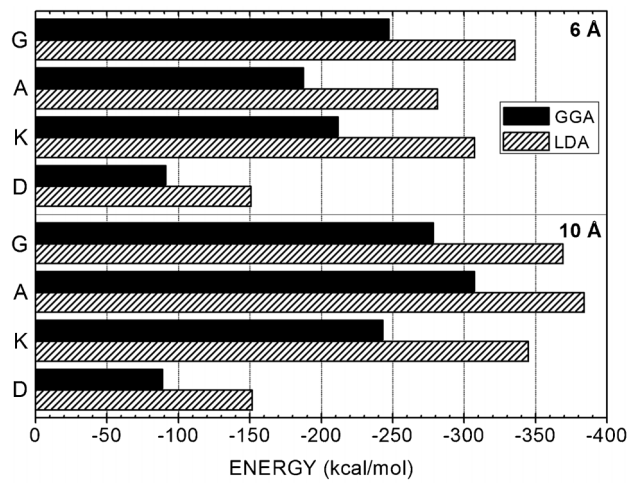

Fig. 3 Total electronic binding energies considering 6 and 10 Å radii. G stands for glutamate, A for AMPA, K for kainate and D for DNQX.

Table 2 Experimental data of ligands bound to GluR2[5,33,34]

Ligand	Relative efficacy (%)	Domain closure (deg.)
Glutamate	100	19.1–21.1
AMPA	88	20.3–21.0
Kainate	21	13.1
DNQX	—	3.4–6.5

Although there are no experimental values for the interaction energy of protein–ligand, it is possible to make a comparison of the experimental data of the relative efficacy and the closure of the LBD caused by each ligand[33] and the calculated interaction energies. The relative efficacy for the system in question is determined in electrophysiological studies by measuring the maximum ionic current (I_{max}) caused by opening the channel when the ligand is interacting with the LBD as measured by microelectrodes. Such a value is then contrasted with the I_{max} caused by glutamate, the natural agonist, which is used as a reference to estimate the relative efficacy of each binder, determining whether a molecule is a full or partial agonist or an antagonist (if there is no response) of the protein.[34,35] Table 2 shows both the relative efficacy and domain closure experimental data for each ligand. What is expected, correlating the interaction energies with the experimental data, is the following sequence of efficacy/domain closure: AMPA > glutamate > kainate > DNQX, which differs from real measurements only in the order of decreasing relative efficacy, for which glutamate has a larger value than AMPA.

The validity of the MFCC scheme to assess the interaction energy of a ligand with a neutral protein using dispersion corrected DFT was investigated recently by Antony and Grimme[36] for protein–ligand complexes with 3680, 1798, and 1060 atoms. Their results show that in such cases the fractionation approach works well. Improvements in the MFCC method were also carried out in the last few years, such as the capability of performing geometry optimizations,[37] the use of molecular mechanics for long range interactions,[38] the addition of the conductor-like polarizable continuum model,[39] and the electrostatic field-adapted MFCC, which allows one to treat charged systems by adding a description of the surrounding environment through the use of point charges.[40] These developments, once incorporated in our simulations, will hopefully ensure more realistic results in future studies. Truly, the lack of an error estimate algorithm to evaluate the accuracy of fragmentation methods is a cause for concern,[41] but this does not prevent their use, especially because they provide valuable information at relatively low computational cost (in comparison with a full-scale run), detailing the physical interactions in protein–ligand systems and even being employed as a tool to improve the design of new drugs.[42]

The single-point electronic binding energies we have calculated are just a starting point on the long road to obtaining the thermodynamic free energy of binding. To this end, it is necessary first to refine the crystallographic data and to find the right protonation pattern of the protein–ligand structure. Afterwards, it will be required to include a modelling of solvation (including water molecules and counterions) and the entropy of the system which does not exist yet for the theoretical approach we adopt in this work. Nevertheless, one can note that current approaches connecting structural information to the free energy of binding are all dependent on empirical data. On the other hand, the gas phase interaction energy estimated from our computations is a fundamental part of the free energy of binding, which means that they give information on one particular step to calculate it and represent an independent check for parts of empirical scoring functions or force fields employed in free energy perturbation estimates.[36]

In summary, our results reinforce the usefulness of computer simulations at the quantum level to understand the GluR2–ligand interaction, allowing one to differentiate, through the comparison of interaction energy values, the agonists, partial agonists and antagonist molecules. Thus, theoretical simulations combining DFT theory with fragmentation methods can be helpful for the development of new drugs targeting the GluR2 receptor. We also demonstrate the necessity of taking into account a larger binding pocket size, including more distant amino acid residues, in order to obtain a good correlation between the simulation and experimental data on the agonist/antagonist action of the ligand. Arg485 is the most important residue for the GluR2–ligand interaction for all the ligand molecules investigated. For the GluR2–glutamate interaction, other important residues are Ser654, Thr655, Leu650, Lys730, Lys656, Glu657 and Asp651; for GluR2–AMPA, Ser654, Thr655, Lys730, Lys656, Lys449, Arg684, Glu402 and Asp651; for GluR2–kainate Ser656, Glu402, Glu657 and Asp651; finally, for GluR2–DNQX the most important residues after Arg485 are Pro478, Glu705 and Leu498.

V. N. Freire and P. de Lima-Neto are senior researchers from the Brazilian National Research Council (CNPq) and thank the financial support received from the CNPq project 301746/2011-7 and from the CNPq-INCT Rede Nano (Bio) Simes project 573924/2008-9. E. W. S. C. received financial support from the CNPq projects 304283/2010-0 and 474734/2011-0. C. G. received financial support from the CNPq project 478916/2010-8. Finally, A. C. V. Martins thanks CAPES for her post-graduate scholarship.

Notes and references

1 D. R. Madden, *Nat. Rev. Neurosci.*, 2002, **3**, 91–101.
2 W. Tichelaar, M. Safferling, K. Keinänen, H. Stark and D. R. Madden, *J. Mol. Biol.*, 2004, **344**, 435–442.
3 C. Rosenmund, Y. Stern-Bach and C. F. Stevens, *Science*, 1998, **280**, 1596–1599.
4 S. F. Traynelis, L. P. Wollmuth, C. J. McBain, F. S. Menniti, K. M. Vance, K. K. Ogden, K. B. Hansen, H. Yuan, S. J. Myers and R. Dingledine, *Pharmacol. Rev.*, 2010, **62**, 405–496.
5 N. Armstrong and E. Gouaux, *Neuron*, 2000, **28**, 165–181.
6 J. Pøhlsgaard, K. Frydenvang, U. Madsen and J. S. Kastrup, *Neuropharmacology*, 2011, **60**, 135–150.
7 N. Armstrong, Y. Sun, G.-Q. Chen and E. Gouaux, *Nature*, 1998, **395**, 913–917.
8 Y. Arinaminpathy, M. S. P. Sansom and P. C. Biggin, *Biophys. J.*, 2002, **82**, 676–683.
9 M. Kubo, E. Shiomitsu, K. Odai, T. Sugimoto, H. Suzuki and E. Ito, *Proteins: Struct., Funct., Genet.*, 2004, **54**, 231–236.
10 K. Speranskiy and M. Kurnikova, *Biochemistry*, 2005, **44**, 11508–11517.
11 Y. Arinaminpathy, M. S. Sansom and P. C. Biggin, *Mol. Pharm.*, 2006, **69**, 11–18.
12 A. Y. Lau and B. Roux, *Structure*, 2007, **15**, 1203–1214.
13 T. Mamonova, K. Speranskiy and M. Kurnikova, *Proteins: Struct., Funct., Bioinf.*, 2008, **73**, 656–671.
14 R. Vijayan, M. A. Sahai, T. Czajkowski and P. C. Biggin, *Phys. Chem. Chem. Phys.*, 2010, **12**, 14057–14066.
15 P. A. Postila, M. Ylilauri and O. T. Pentikäinen, *J. Chem. Inf. Model*, 2011, **51**, 1037–1047.
16 O. Okada, K. Odai, T. Sugimoto and E. Ito, *Biophys. Chem.*, 2012, **162**, 35–44.
17 M. Kubo, K. Odai, T. Sugimoto and E. Ito, *J. Biochem.*, 2001, **129**, 869–874.
18 M. Kubo, E. Shiomitsub, K. Odai, T. Sugimoto, H. Suzukib and E. Ito, *THEOCHEM*, 2003, **634**, 145–157.
19 M. Kubo, E. Shiomitsub, K. Odai, T. Sugimoto, H. Suzukib and E. Ito, *THEOCHEM*, 2003, **639**, 117–128.
20 K. Odai, T. Sugimoto, M. Kubo and E. Ito, *J. Biochem.*, 2003, **133**, 335–342.
21 M. A. Sahai and P. C. Biggin, *J. Phys. Chem. B*, 2011, **115**, 7085–7096.
22 G. Zanatta, I. L. Barroso-Neto, V. Bambini-Junior, M. F. Dutra, E. M. Bezerra, R. F. da Costa, E. W. S. Caetano, B. S. Cavada, V. N. Freire and C. Gottfried, *J. Proteo. Bioinf.*, 2012, **5**, 155–162.
23 I. L. Barroso-Neto, J. P. C. Marques, R. F. da Costa, E. W. S. Caetano, B. S. Cavada, C. Gottfried and V. N. Freire, *J. Phys. Chem. B*, 2012, **116**, 3270–3279.
24 R. F. da Costa, V. N. Freire, E. M. Bezerra, B. S. Cavada, E. W. S. Caetano, J. L. de Lima-Filho and E. L. Albuquerque, *Phys. Chem. Chem. Phys.*, 2012, **14**, 1389–1398.
25 M. P. Allen and D. J. Tildesley, *Computer Simulation of Liquids*, London, Clarendon Press, Oxford Science Publications,1987.
26 S. Lifson, A. T. Hagler and J. P. Stockfisch, *J. Am. Chem. Soc.*, 1979, **101**, 5111–5121.
27 P. Dauber-Osguthorpe, V. A. Roberts, D. J. Osguthorpe, J. Wolff, M. Genest and A. T. Hagler, *Proteins: Struct., Funct., Genet.*, 1988, **4**, 31–47.
28 B. Delley, *J. Chem. Phys.*, 1990, **92**, 508–517.
29 B. Delley, *J. Chem. Phys.*, 2000, **113**, 7756–7764.
30 J. P. Perdew and Y. Wang, *Phys. Rev. B: Condens. Matter*, 1992, **46**, 12947–12954.
31 J. P. Perdew, K. Burke and M. Ernzerhof, *Phys. Rev. Lett.*, 1996, **77**, 3865–3868.
32 A. Tkatchenko and M. Scheffler, *Phys. Rev. Lett.*, 2009, **102**, 073005.
33 J. Pøhsgaard, K. Frydenvang, U. Madsen and J. S. Kastrup, *Neuropharmacology*, 2011, **60**, 135–150.
34 A. Frandsen, D. S. Pickering, B. Vestergaard, C. Kasper, B. B. Nielsen, J. R. Greenwood, G. Campiani, C. Fattorusso, M. Gajhede, A. Schousboe and J. S. Kastrup, *Mol. Pharmacol.*, 2005, **67**, 703–713.

35 H. P. Rang, *Br. J. Pharmacol.*, 2006, **147**, S9–S16.
36 J. Antony and S. Grimme, *J. Comput. Chem.*, 2012, **33**, 1730–1739.
37 S. H. Li, W. Li and T. Fang, *J. Am. Chem. Soc.*, 2005, **127**, 7215–7226.
38 X. He and J. Z. H. Zhang, *J. Chem. Phys.*, 2006, **124**, 184703.
39 Y. Mei, C. G. Ji and J. Z. H. Zhang, *J. Chem. Phys.*, 2006, **125**, 094906.
40 N. Jiang, J. Ma and Y. Jiang, *J. Chem. Phys.*, 2006, **124**, 114112.
41 M. S. Gordon, D. G. Fedorov, S. R. Pruitt and L. V. Slipchenko, *Chem. Rev.*, 2012, **112**, 632–672.
42 O. Ichihara, J. Barker, R. J. Law and M. Whittaker, *Mol. Inf.*, 2011, **30**, 298–306.

